IOP PUBLISHING JOURNAL OF PHYSICS B: ATOMIC, MOLECULAR AND OPTICAL PHYSICS

J. Phys. B: At. Mol. Opt. Phys. **40** (2007) 3143–3152 doi:10.1088/0953-4075/40/15/013

Thermalization of magnetized electrons from black body radiation

F Robicheaux[1] **and J Fajans**[2]

[1] Department of Physics, Auburn University, AL 36849-5311, USA
[2] Department of Physics, University of California at Berkeley, Berkeley, CA 94720-7300, USA

Received 23 May 2007, in final form 24 June 2007
Published 25 July 2007
Online at stacks.iop.org/JPhysB/40/3143

Abstract
We describe an interesting mechanism whereby an electron in a strong magnetic field can have both the parallel and perpendicular motions come into thermal equilibrium with black body radiation. The mechanism does not include any collisions with other particles and can overcome the extreme slowing of thermalization of highly magnetized particles at low temperatures. The mechanism depends upon the magnetic field strength having a spatial variation. We provide results from two example cases. This mechanism could affect the temperatures that can be achieved in experiments devoted to trapping antihydrogen.

1. Introduction

The approach to thermal equilibrium is a complicated process for non-neutral plasmas in a magnetic field. As an example of this, O'Neil and Hjorth [1] showed that the motions of an electron perpendicular and parallel to a magnetic field essentially decouple at low temperatures and high magnetic fields. A more accurate expression for the rate and a comparison with the experiment have been provided in [2]. The decoupling arises due to an adiabatic invariant and it holds even for the multiple interactions in a plasma. Thus, collisions redistribute energy between the parallel and perpendicular motions in a cold, highly magnetized plasma only on very long time scales.

Recently, two groups [3, 4] reported the formation of antihydrogen ($\bar{\mathrm{H}}$) by having anti-protons ($\bar{\mathrm{p}}$) traverse a positron (e^+) plasma. The next goal [5] is to have the antihydrogen form in a manner where it can be trapped. In these experiments, the positron and electron plasmas are highly magnetized and cold. The electron plasmas are present to cool the anti-protons while the positron plasma is present for the formation of anti-hydrogen.

It is thought that the plasmas in [3, 4] were in thermal equilibrium with the black body radiation. The photons couple to the cyclotron motion giving thermalization of the motion perpendicular to the magnetic field on the $\sim$1 s time scale while collisions will couple the parallel and perpendicular motions. For the experimental parameters, the cyclotron motion couples much more strongly to the radiation field than the motion along the magnetic field. If the electrons or positrons start at a higher temperature than the radiation field, the cyclotron motion tends to radiate away energy but the temperature along the field is unchanged unless the collision rate is large enough to couple the perpendicular and parallel motions. However, the coupling rate strongly decreases with temperature at low temperatures so that we can expect that the parallel motion could have a substantially higher temperature than the cyclotron motion. Conversely, if the electrons or positrons start at a lower temperature than the radiation field, the cyclotron motion tends to absorb energy. In this case, the parallel motion could end up substantially cooler than the cyclotron motion. For the reported parameters, the computed thermalization time [1] due to collisions is comparable to or longer than the experimental time scales. Thus, we were led to investigate whether other mechanisms might provide faster thermalization than collisions.

From [2], the thermalization rate between the two motions can be written as

$$\Gamma = n\bar{b}^2\bar{v}_{\parallel}I(\bar{\kappa}), \tag{1}$$

where n is the positron or electron density, $\bar{b} = 2e^2/(4\pi\varepsilon_0 k_B T_{\parallel})$ gives the scale length and $\bar{v}_{\parallel} = \sqrt{k_B T_{\parallel}/\mu}$ gives the scaled velocity with $\mu = m/2$ as the reduced mass. The parameter $\bar{\kappa} = \Omega\bar{b}/\bar{v}_{\parallel}$ with the cyclotron frequency, $\Omega = eB/m$, is a dimensionless number which is proportional to the ratio of the collision time to the cyclotron period. For a cold, highly magnetized plasma, $\bar{\kappa}$ is a large number. From [2], the function I can be approximated as

$$I(\bar{\kappa}) = \left(\frac{1.83}{\bar{\kappa}^{7/15}} + \frac{20.9}{\bar{\kappa}^{11/15}} + \frac{0.347}{\bar{\kappa}^{13/15}} + \frac{87.8}{\bar{\kappa}^{15/15}} + \frac{6.68}{\bar{\kappa}^{17/15}}\right)\exp\left(-[5/6](3\pi\bar{\kappa})^{2/5}\right). \tag{2}$$

To see how strong the effect is we compute the rate for a few relevant parameters. For parameters similar to those reported for the ATHENA experiment [3], $T = 15$ K, $B = 3$ T and $n_e = 10^8$ cm^{-3}, the thermalization rate is $\Gamma \sim 1$ kHz. For parameters similar to those reported for the ATRAP experiment [4], $T = 4$ K, $B = 5$ T and $n_e = 10^7$ cm^{-3}, the thermalization rate is $\Gamma \sim 3 \times 10^{-6}$ Hz. These numbers suggest that the plasma is collisionally thermalized for the ATHENA experiment but not for the ATRAP experiment. For $T = 1$ K, $B = 2$ T and $n_e = 10^7$ cm^{-3}, the thermalization rate is $\Gamma \sim 1 \times 10^{-12}$ Hz.

For a uniform magnetic field, the photons do not bring the parallel motion into thermal equilibrium quickly. There are two mechanisms which could do this, but both are slow. There is acceleration of the electron or positron along the magnetic field due to electric fields; this acceleration can couple to the radiation field. However, the frequencies are roughly MHz compared to the ∼30–200 GHz cyclotron motion and thus the rate of photon absorption is extremely slow and the photon energies are tiny. A second mechanism is from the momentum kicks when photons with energy $\hbar\Omega$ are absorbed or emitted. Unfortunately, the photon momentum is too small to provide substantial changes. For example, in a 1 T field, the cyclotron frequency is 28 GHz which corresponds to photons with momentum 6.17×10^{-32} kg m s^{-1}: each time a photon is absorbed or emitted an electron has a change of velocity of 0.068 m s^{-1} compared to the ∼10 000 m s^{-1} speeds for a temperature of several K. Since photons are absorbed and emitted with rates on the order of Hz, there is a negligible change of electron momentum along the magnetic field.

In this paper, we investigate a third mechanism for bringing the parallel and perpendicular motions into equilibrium with the radiation field. The idea is similar to that described in [6, 7]. In these papers, the antihydrogen centre-of-mass motion cools as it moves through a spatially varying magnetic field while it radiatively cascades. The basic idea is that the magnetic moment decreases with time which means the antihydrogen experiences a centre-of-mass force which has an overall decrease with time. A similar circumstance occurs when a positron or electron moves through a spatially varying magnetic field. The overall potential it experiences depends on the number of quanta in the cyclotron motion. The electron or positron experiences a potential of the form $U(z)+2(n+1/2)\mu_B B(z)$, where n is the number of quanta in the cyclotron motion, z parametrizes the motion along the magnetic field, $\mu_B = e\hbar/2m$ is the Bohr magniton, $B(z)$ is the magnitude of the magnetic field and $U(z)$ is an external (usually electrostatic) potential. Thus, as the electron or positron absorbs/emits photons, the number of quanta in the cyclotron motion, n, changes and the centre-of-mass force fluctuates. This leads to momentum kicks along the magnetic field which can help bring this motion into thermal equilibrium.

To see how this works, first consider the case where a positron has much more energy in the cyclotron motion than the thermal black body energy, $k_B T_{bb}$. In this situation, the positron will tend to emit photons. Since the positron spends most of the orbital time near its turning points, that is where it will tend to emit photons. If the magnetic field has a minimum near the minimum of the electrostatic potential, the positron tends to lose kinetic energy along the magnetic field with each photon emission because the energy that would be acquired as it moves to lower $B(z)$ will be less after the photon emission. Conversely, if the positron starts with energy much less than $k_B T_{bb}$ in the cyclotron motion, it will tend to absorb photons. Now, it will tend to absorb photons near the turning point and gain extra energy as it moves to lower $B(z)$. In this case, the kinetic energy along the field will tend to increase. When the energy in the cyclotron motion is approximately $k_B T_{bb}$, the number of absorptions and emissions are roughly equal. In this case, whether the positron gains or loses energy depends on the kinetic energy of the positron. On average, the kinetic energy of the positron will approach $k_B T_{bb}/2$ and the rate that it approaches this value depends on the fluctuations in the force that arises from the $2(n + 1/2)\mu_B B(z)$ part of the potential. We will discuss this situation in more detail below.

For the anti-hydrogen experiments, there are three other mechanisms that could lead to thermalization of the motion along the magnetic field. Unfortunately, all three have significant uncertainties which does not allow us to say whether they are important.

(1) The electron and positron motion along the field oscillates with a frequency of ∼MHz. The wavelength of light at this frequency is much larger than the distance to the walls of the trap. Thus, the electron or positron can directly couple to the walls of the trap through electrostatic interactions. We are uncertain how to estimate the size of this effect due to the complications of the geometry, the material (gold-plated aluminium electrodes), the high magnetic field and the low temperature.

(2) The electrons and positrons are usually in a plasma and the plasma has surface and density waves that could couple to the motion along the magnetic field. Unfortunately, the temperature of the plasma modes is not a known quantity.

(3) Collisions with particles of a different type could couple the cyclotron motion and the motion along the B-field. For example, anti-protons pass through the positron plasma and the electrons are used to cool anti-protons. An anti-proton collision with an electron does not couple the parallel and perpendicular motions of the electron effectively because the electron does not closely approach the anti-proton. However, an anti-proton collision with a positron can couple the two motions because a close collision is allowed. We do not know of existing data that could be used to estimate this rate. If we estimate the rate from $\pi r^2 v$ with r the cyclotron radius and v the thermal velocity, we get a rate of $\sim 10^{-4}$ cm ^{3} s^{-1} in a 1 T field. The density of anti-protons in the region of the positrons has been in the range of 10^1–10^4 cm^3, depending on the geometry and the number of trapped anti-protons. The upper end of this range gives time scales comparable to those in this paper.

For the rest of this paper, we will refer to the charged particle as an electron for simplicity. All of the results apply equally well to positrons.

2. Basic theory and approximations

To completely treat all of the motions of the electron through a spatially varying magnetic field is beyond the scope of computational resources. This necessitates the use of various approximations whose accuracy is discussed in this section.

We will treat the motion of the electron along the magnetic field using a classical approximation. This should be very accurate for all of the parameters discussed in this paper. For example, the de Broglie wavelength of an electron at 1 K is roughly 200 nm whereas the distance scale is approximately cm. Thus, there are approximately 10^4–10^5 wavelengths within the bounded region which means the correspondence principle should lead to accurate results from a classical simulation.

We treat the motion of the electron perpendicular to the magnetic field in a purely quantum treatment. For a constant B-field in the z-direction the Hamiltonian in atomic units is

$$H = \frac{p_x^2 + p_y^2}{2} + \frac{\gamma}{2} L_z + \frac{\gamma^2}{8}(x^2 + y^2), \tag{3}$$

where $\gamma = B/2.35 \times 10^5$ T is the magnetic field strength in atomic units. By using the operators,

$$A_\pm = \frac{1}{\sqrt{2}} \left(\frac{\sqrt{\gamma}}{2}[x \mp \mathrm{i}y] + \frac{\mathrm{i}}{\sqrt{\gamma}}[p_x \mp \mathrm{i}p_y] \right) \tag{4}$$

one can show that $\left[A_\pm, A_\pm^\dagger\right] = 1$, $\left[A_\mp, A_\pm^\dagger\right] = 0$, $L_z = A_+^\dagger A_+ - A_-^\dagger A_-$ and

$$H = \gamma\left(A_+^\dagger A_+ + 1/2\right). \tag{5}$$

Note that the energies do not depend on the number of '$-$' quanta. This means that the energy levels are given by $E_n = (n_+ + 1/2)\gamma$. In SI units, the energy levels are given by $E_n = (n_+ + 1/2)\hbar eB/m$ where m is the mass of the electron. The spontaneous decay rate to go from $n_+ \to n_+ - 1$ is given by

$$\Gamma_{n_+} = \frac{4\alpha^3\gamma^2}{3} n_+ \tag{6}$$

in atomic units with α the fine structure constant. In SI units, the rate is given by

$$\Gamma_{n_+} = \frac{4e^4B^2}{12\pi\varepsilon_0 c^3 m^3} n_+, \tag{7}$$

which can be simplified to $\Gamma_{n_+} = 0.384 B^2 n_+$ Hz if B is in T. Since the energy levels and the decay rate only depend on n_+, we will simplify the notation by relabelling $n_+ \to n$ where n will denote the quantum level.

When there is a black body radiation field at temperature T_{bb} present, the decay rate is modified and photon absorption becomes possible. The rate for emitting a photon is

$$\Gamma_{n\to n-1} = n\Gamma_1 s/(s-1), \tag{8}$$

where Γ_1 is from equation (7) and $s = \exp(\hbar\Omega/k_{\mathrm{B}}T_{\mathrm{bb}}) = \exp(\hbar eB/[mk_{\mathrm{B}}T_{\mathrm{bb}}])$. The rate for absorbing a photon is

$$\Gamma_{n\to n+1} = (n+1)\Gamma_1/(s-1). \tag{9}$$

For an electron in thermal equilibrium with the black body radiation field, the average number of excitation quanta is $\langle n \rangle = 1/(s-1)$. For an electron at 4 K in a 2 T field, $\langle n \rangle \simeq 1.0$. For an electron at 4 K in a 5 T field, $\langle n \rangle \simeq 0.23$. Thus, the perpendicular motion of the electron can not be considered classically for these cases; the second case is for reported ATRAP parameters and shows that the electrons in their plasma were mostly in the ground state for the cyclotron motion.

Because there are so few quanta in the cyclotron motion, the spin of the electron could also play a role. The spin can flip through the photon emission and absorption. However, the rate for this is several orders of magnitude lower than for the cyclotron motion. The reason is that the spin flips go through magnetic dipole transitions but the cyclotron motion changes n through electric dipole transitions. Since the spin will rarely flip, we will ignore this effect.

In this paper, we consider the case of spatially varying magnetic fields. Thus, the discussion of the previous paragraphs will only be approximately correct for our simulations. There are two approximations that we make. We treat the magnetic field as being constant over a cyclotron orbit. For a 4 K electron in a 1 T field, the cyclotron radius is ~100 nm while the B-field varies over centimetre size scales. The second approximation is that we will say that the motion of the electron along the field does not cause transitions between the quantum states. The cyclotron frequency is in the 10–100 GHz range whereas the variation time of the magnetic field is 10^4 m/s/1 cm ~ MHz. Since the magnetic moment is an adiabatic invariant, these will both be excellent approximations.

To simulate the evolution of the electron properties, we utilize a Monte Carlo technique. We treat the motion along the magnetic field as a one-dimensional motion given by the classical Hamiltonian

$$H_{\mathrm{cl}} = \frac{p^2}{2m} + U(z) + 2(n + 1/2)\mu_B B(z), \tag{10}$$

where z parametrizes the motion along the magnetic field, $\mu_B = e\hbar/2m$ is the Bohr magniton, $B(z)$ is the magnitude of the magnetic field and $U(z)$ is an external (usually electrostatic) potential. The equations of motion are given by

$$\dot{z} = p/m \qquad \dot{p} = -\frac{\partial U(z)}{\partial z} - (2n + 1)\mu_B \frac{\partial B(z)}{\partial z}. \tag{11}$$

The motion along z is solved for classically using this equation during a small interval δt. After the time step, the photon emission and absorption rate are computed at that position. The probability that n increases by 1 is given by $\Gamma_{n\to n+1}\delta t \ll 1$ and the probability that it decreases by 1 is given by $\Gamma_{n\to n-1}\delta t \ll 1$. To determine which (if either) happens, we generate a random number and compare to each of these probabilities. If a photon is absorbed or emitted, the electron sees a new effective force. It is this fluctuation of the force along the magnetic field that gives thermalization.

3. Results

In this section, we present the results from two different cases. In the first case, we will remove the extra potential $U(z)$ so that the range of motion of the electron is completely determined by the increasing magnetic field. This will give the maximum rate for transitions. For the second case, we will have the motion along the field mainly determined by $U(z)$ with only a little change due to the magnetic field. This case will mostly resemble that seen in proposed antihydrogen experiments. Here the effect is small but is still larger than that from collisions.

For all of the calculations in this section, the black body radiation is at 4 K.

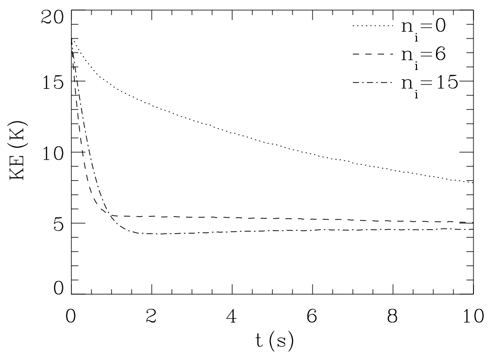

Figure 1. The average kinetic energy at $z = 0$ for an electron distribution that initially has KE = 18 K. The dotted line is when all of the electrons start with $n = 0$, the dashed line is for $n = 6$ and the dash-dot line is for $n = 15$. The only processes included in the calculation is the motion of the electron along a spatially varying magnetic field and the fluctuating magnetic dipole moment due to emission and absorption of photons. There is no electrostatic potential to provide a restoring force. See the text for details.

3.1. No electrostatic forces

For this situation, we will take $U(z)$ to be 0. The motion in z will be confined solely by the magnetic field. To facilitate the calculations, we will take a particularly simple form for B,

$$B(z) = B_0 \times \left(1 + \left[\frac{z^2}{\Delta z^2}\right]\right). \tag{12}$$

This form of B gives harmonic motion along z with a frequency that fluctuates due to the photon emission and absorption. For all of the calculations in this section, we have taken $B_0 = 2$ T and $\Delta z = 1$ cm. This means that the period of motion is always less than 10 μs.

In figure 1, we show the average kinetic energy of the electron as it passes through $z = 0$ as a function of time. For this set of calculations we started with an initial kinetic energy of 18 K. The dotted line shows the average kinetic energy when the electron started with $n = 0$ at $t = 0$. The dashed line is when $n = 6$ at $t = 0$; this corresponds to 17 K of cyclotron energy at 2 T. The dash-dot line is when $n = 15$ at $t = 0$. There is clearly a different behaviour among these three cases. It arises due to the initial radiative cascade. The average number of quanta is roughly 1 at 4 K. Therefore, during the first ~1 s, the electron is more likely to emit photons than absorb photons for the case where n starts at 6 or 15. For these two cases, the effective potential along B appears to be opening up, giving an adiabatic cooling effect. This is the same effect that gives centre-of-mass cooling to the antihydrogen as discussed in [6]. This effect is substantial, causing a loss of over 10 K in KE along the magnetic field. After the initial radiative cascade, the fluctuating potential from multiple emission and absorptions begins to bring the distribution towards thermal equilibrium. The case that starts with $n = 0$ does not show the fast initial drop. However, the KE has decreased by a factor of 2 even in this situation. Thus, the spatially varying magnetic field is an effective mechanism for bringing the motion along the field into thermal equilibrium without collisions.

Because the photon emission and absorption rate increase with the number of quanta, n, in the cyclotron motion, the total number of photons emitted and absorbed is highest with the $n = 15$ starting condition. During the 10 s shown in figure 1, the average number of emissions and absorptions is 37 for $n_i = 0$, 66 for $n_i = 6$ and 94 for $n_i = 15$.

In figure 2, we show the distribution of kinetic energies for the situation in figure 1. The solid line shows a thermal distribution for a temperature of 4 K. The $t = 0$ distribution

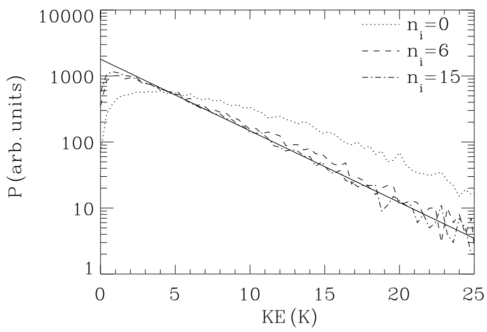

Figure 2. The distribution of KE at $t = 10$ s for the conditions of figure 1. The line types correspond to that in figure 1. The solid line is proportional to a thermal distribution at 4 K.

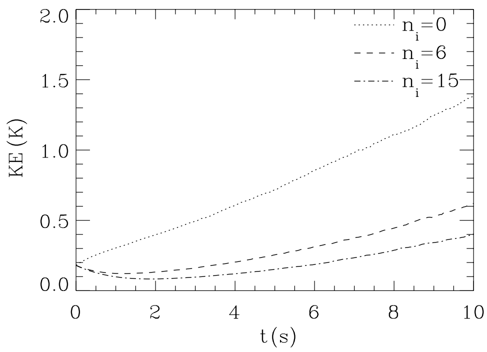

Figure 3. The same as figure 1 but for a starting KE = 0.18 K.

shows a sharp peak at 18 K. The distributions at the final time, 10 s, are shown for the $n = 0$ starting condition (dotted line) the $n = 6$ starting condition (dashed line), and the $n = 15$ starting condition (dash-dot line). These distributions are computed from the kinetic energy of each atom as it crosses the $z = 0$ point for the first time after $t = 10$ s. It is clear that the $n = 6$ and $n = 15$ are already in qualitative agreement with a thermal distribution. The main difference is for small KE where the distribution has much less population than purely thermal. The low-energy part of the distribution is the slowest to thermalize because the size of the fluctuating force decreases with decreasing energy. In the extreme case of KE = 0, the electron would not gain energy from this mechanism because the potential does not fluctuate at all when the electron is confined to $z = 0$. The $n = 0$ distribution does not look much like a thermal distribution at $t = 10$ s. But by 30 s, the distribution is qualitatively thermal. We have also performed calculations out to 100 s and found that the distributions become excellent approximations to a thermal distribution over that time scale.

We repeated the calculation but for a starting kinetic energy that was 1/100 that of figures 1 and 2. In figure 3, we show the average kinetic energy but with electrons starting with 0.18 K of kinetic energy at $t = 0$. There are many features that are similar to that in figure 1. For example, the $n = 6$ and $n = 15$ starting conditions give an initial drop in kinetic energy. However, the rate for approaching ∼4 K is clearly slower than in figure 1. The reason is that the lower kinetic energy means the size of the fluctuating part of the potential is smaller. During the 10 s shown in figure 1, the average number of emissions and absorptions is 64 for $n_i = 0$, 82 for $n_i = 6$ and 110 for $n_i = 15$.

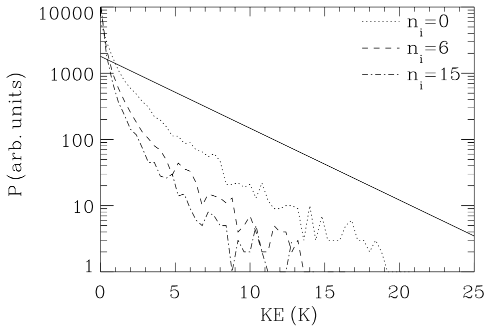

Figure 4. The same as figure 2 but for a starting KE = 0.18 K.

Figure 4 is similar to figure 2 but for the lower starting kinetic energy. Again, it is clear that the distribution approaches a thermal distribution much more slowly than when starting from higher kinetic energy. The low-energy part of the distribution changes slowly. Once the fluctuations cause the electron to reach energies above ∼1 K, the energy changes become more rapid. The time scale for this thermalization is much shorter than from collisions; the collisional thermalization for a 1 K plasma in a 2 T field has a rate of $\sim 10^{-12}$ Hz for a density of 10^7 cm^{-3}.

3.2. Large electrostatic forces

The previous example shows that thermalization from a spatially varying magnetic field could be an important effect in some circumstances. In this section, we choose parameters that are more nearly like those in the antihydrogen experiments. In these experiments, electrostatic potentials confine the electron plasma to a region near the centre of the trap. Because the plasma is cold, the total potential is very flat across the whole of the plasma and then it rises sharply near the edge. Also, it is mirror coils that produce the magnetic field that rises away from the middle of the plasma.

To model the full electrostatic potential, we chose a potential with the form

$$U(z) = \mathrm{KE}_0 \times \left(\frac{z}{\Delta z}\right)^{10}, \tag{13}$$

where KE_0 is a parameter with units of energy and Δz sets the size of the plasma. In all of the simulations, we chose KE_0 to equal the starting kinetic energy of the electron along the field and Δz is half the width of the plasma.

The magnetic field was chosen to be the sum of a uniform magnetic field and the field from two single loop coils. We chose the form

$$B(z) = B_0 + B_{\mathrm{mirr}} \left[\frac{r^3}{(r^2 + (z - z_{\mathrm{mirr}})^2)^{3/2}} + \frac{r^3}{(r^2 + (z + z_{\mathrm{mirr}})^2)^{3/2}}\right], \tag{14}$$

where B_0 is the strength of the uniform field, B_{mirr} is the strength of the magnetic field from one loop at its centre, r is the radius of the loop and z_{mirr} is the distance from the centre of the plasma to the mirror. This gives a magnetic field symmetric in z that increases away from $z = 0$. For the calculations in this section, we chose $B_0 = B_{\mathrm{mirr}} = 2$ T, $r = 4.06$ cm and $z_{\mathrm{mirr}} = 12$ cm.

In figure 5, we show the time evolution of the average electron kinetic energy at $z = 0$ for an initial kinetic energy of 18 K. We chose the length of the plasma to be $\Delta z = 5$ cm; most

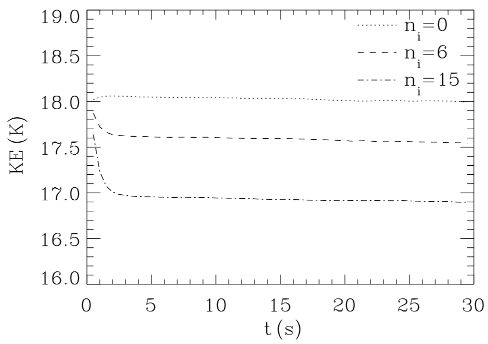

Figure 5. The same as figure 1 but for the case where the magnetic field does not vary strongly over the region of electron motion. Nearly all of the restoring force is provided by an electrostatic potential that rises sharply. See the text for details.

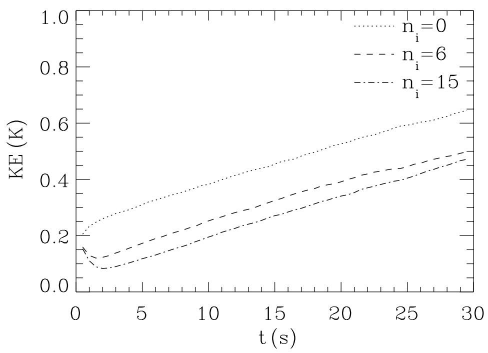

Figure 6. The same as figure 5 but for a starting KE = 0.18 K.

of the reported plasmas have smaller Δz. It is clear that the size of the effect has decreased dramatically. This is because most of the force is from the electrostatic potential which does not fluctuate with the absorption and emission of photons. Also, the form of the potential is such that the electron more sharply reverses directions at the end of the range; thus a smaller fraction of the time is spent at large $|z|$ where the fluctuations are largest. An absorption or emission at $z = \pm 5$ cm corresponds to a change of kinetic energy at the origin of ~ 0.1 K for absorption and ~ -0.1 K for emission. The two cases that start with $n > 0$ give an initial rapid drop in KE as before although the size is reduced.

Figure 6 shows the same parameters as figure 5 but for a starting kinetic energy of 0.18 K. Again it is clear that there is not much change in energy. However, the change is *much* larger than would arise from collisional coupling between the perpendicular and parallel motions.

Figures 5 and 6 indicate this mechanism may not be important for the antihydrogen experiments. But before dismissing this mechanism altogether, we must be somewhat cautious. We have chosen an example of magnetic fields to reduce the size of this effect as much as possible. There are situations consistent with current antihydrogen experiments that would give larger rates. For example, a larger fluctuating force and a more rapid thermalization would result if the size of the uniform field was reduced but the field for the mirror coils was raised. Also, we have only considered the simplest possible case to explore: thermalization only through the radiation field. It might be that this mechanism combined with electron–electron collisions gives much faster thermalization. Finally, it is not clear what the final form of these experiments will be. There are other scenarios under consideration [8] that may give larger thermalization rates than those presented in this section.

4. Conclusions

We performed calculations that demonstrated how spatially varying magnetic fields could cause the motion along the magnetic field to come into thermal equilibrium without collisions. The size of the effect can be quite large if most of the confinement of the motion is from the magnetic field. We expect the effect to be slower for the experiments attempting to trap antihydrogen. However, this assessment depends on the particular parameters in the experiment. We can easily envision cases where this effect can be important. For example, we chose a case where the magnetic field hardly changes over the region of motion.

The largest limitation of our calculation was the neglect of collisions. The electrons are in a cold plasma. Imagine two electrons A and B that start with the same energy and have quantum number $n = 0$. Suppose A then absorbs a photon and so has higher kinetic energy. After a collision, A and B exchange kinetic energy but not excitation. Now A is in a higher quantum state but B has the extra kinetic energy. Later, A emits a photon to get back into its original quantum state. It is unclear to us whether this will cause a faster thermalization than the case without collisions. Unfortunately, the simulation of such a complicated series of interactions seems to be beyond what can be handled by our computational resources.

Finally, we will mention a more speculative situation. Suppose that instead of the black body radiation field, the radiation field has an additional weak component that only causes cyclotron transitions at the magnetic field minimum. When the electrons are cold enough so that the average number of quanta in the cyclotron motion, $\langle n \rangle$ is less than one, then the extra field will cause more transitions that increase n than decrease n. However, the electron is more likely to radiate at the regions of higher B. This will provide a net cooling. It may be possible to send in microwaves for $\sim$10 s to cool the motion along the magnetic field. After the microwaves are turned off, the cyclotron motion quickly cools to the temperature of the black body radiation. This could give colder electrons than would otherwise obtain.

Acknowledgments

We acknowledge insightful discussions with J D Hanson. This work was supported by the Office of Fusion Energy, US Department of Energy.

References

[1] O'Neil T M and Hjorth P G 1985 *Phys. Fluids* **28** 3241
[2] Glinsky M E, O'Neil T M, Rosenbluth M N, Tsuruta K and Ichimaru S 1992 *Phys. Fluids* B **4** 1156
[3] Amoretti M *et al* (ATHENA Collaboration) 2002 *Nature* **419** 456
[4] Gabrielse G *et al* (ATRAP Collaboration) 2002 *Phys. Rev. Lett.* **89** 213401
[5] Andresen G *et al* (ATHENA Collaboration) 2007 *Phys. Rev. Lett.* **98** 023402
[6] Zhang J, Taylor C L, Hanson J D and Robicheaux F 2007 *J. Phys. B: At. Mol. Opt. Phys.* **40** 1019
[7] Pohl T, Sadeghpour H R, Nagata Y and Yamazaki Y 2006 *Phys. Rev. Lett.* **97** 213001
[8] Mohri A and Yamazaki Y 2003 *Europhys. Lett.* **63** 207